A CASE STUDY OF THE NOCTURNAL BOUNDARY LAYER OVER A COMPLEX TERRAIN

MATTHEW J. PARKER and SETHU RAMAN*

Environmental Technology Section, Savannah River Technology Center, Westinghouse Savannah River Company, Aiken, South Carolina 29808, U.S.A.

(Received 18 February, 1993)

Abstract. A case study of the structure of the nocturnal boundary layer (NBL) over complex terrain is presented. Observations were made during the third night of Project STABLE (Weber and Kurzeja, 1991), whose main goal was to study turbulence and diffusion over the complex terrain of the Savannah River Site (SRS) near Augusta, Georgia.

The passage of a mesoscale phenomenon, defined as a turbulent meso-flow (TMF) with an explanation of the nomenclature used, and a composite structure of the lowest few hundred meters over complex terrain are presented. The spatial extent of the TMF was at least 30–50 km, but the forcing is not well understood. The TMF occurred without the presence of a synoptic-scale cold front, under clear conditions, and with no discernible discontinuity in a microbarograph pressure trace. The structure of the NBL over the complex terrain at SRS differed from the expected homogeneous terrain NBL. The vertical structure exhibited dual low level wind maxima, dual inversions, and a persistent elevated turbulent layer.

The persistent elevated turbulent layer, with a spatial extent of at least 30 km, was observed for the entire night. The persistent adiabatic layer may have resulted from turbulence induced by shear instability.

1. Introduction

The complex nature of the nocturnal boundary layer (NBL) has been discussed extensively in the literature (Arya, 1988; Stull, 1988). Observations of the mean and turbulent structure of the NBL over an ideal, nearly homogeneous terrain are more common as compared to those over complex terrain. However, observational studies of the NBL over complex terrain, where real, operational atmospheric effluent modeling is necessary, enable the evaluation of NBL modeling schemes against atmospheric data. During three nights in April, 1988, Project STABLE (Weber and Kurzeja, 1991) was undertaken at the Savannah River Site (SRS) near Augusta, Georgia (see Figure 1) to investigate turbulence and diffusion in the NBL over complex terrain to evaluate the SRS atmospheric models. The Savannah River Technology Center (SRTC) conducted the experiment with the participation of the North Carolina State University (NCSU) and Lawrence Livermore National Laboratories (LLNL).

* Department of Marine, Earth, and Atmospheric Sciences, North Carolina State University, Raleigh, North Carolina 27695-8208, U.S.A.

Boundary-Layer Meteorology **66**: 303–324, 1993.

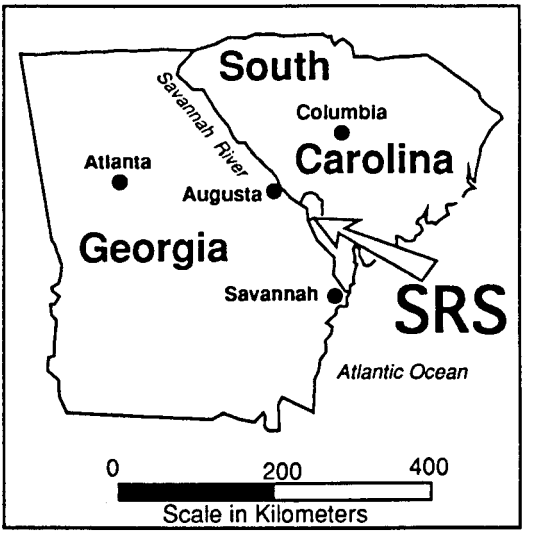

Fig. 1. Location of the Savannah River Site in South Carolina, USA.

The main emphasis of the current study is given to an observed mesoscale feature defined as a "turbulent meso-flow" (TMF), which traveled at least 30–50 km, and to the composite vertical structure which included a persistent elevated turbulent layer and dual low-level wind maxima.

2. Data

During Project STABLE, several systems were used for data collection. Mesoscale features were observed by a permanent array of eight 61 m towers instrumented with Teledyne Geotech bivanes and cup anemometers. Six launches of a tethersonde taken jointly by SRTC and NCSU were made up to about 450 m, measuring wind speed and direction, potential temperature, and specific humidity. Five-second averages of air temperature and wind speed were made from permanent meteorological instrumentation at seven levels of the 304 m WJBF-TV tower near the SRS. NCSU operated instruments mounted at 36 m on the Central Climatology tower (CC). NCSU operated a Campbell Scientific one-dimensional sonic anemometer and a fine wire thermocouple to obtain the $\overline{w'T'}$ covariance for turbulent heat flux calculations as well as standard deviations of temperature (σ_T, °C) and vertical velocity (σ_W, m s^{-1}). NCSU also obtained standard deviations of wind direction (σ_A, deg) from a Gill u, v, w propeller anemometer. The instruments were mounted on a 1.3 m boom approximately 0.4 m apart. The sampling rate for NCSU's equipment was 10 Hz with an averaging period of one hour ending on the hour. Post analyses include data from the nearby Plant Vogtle nuclear power plant observation tower and from the National Weather Service at Bush Field

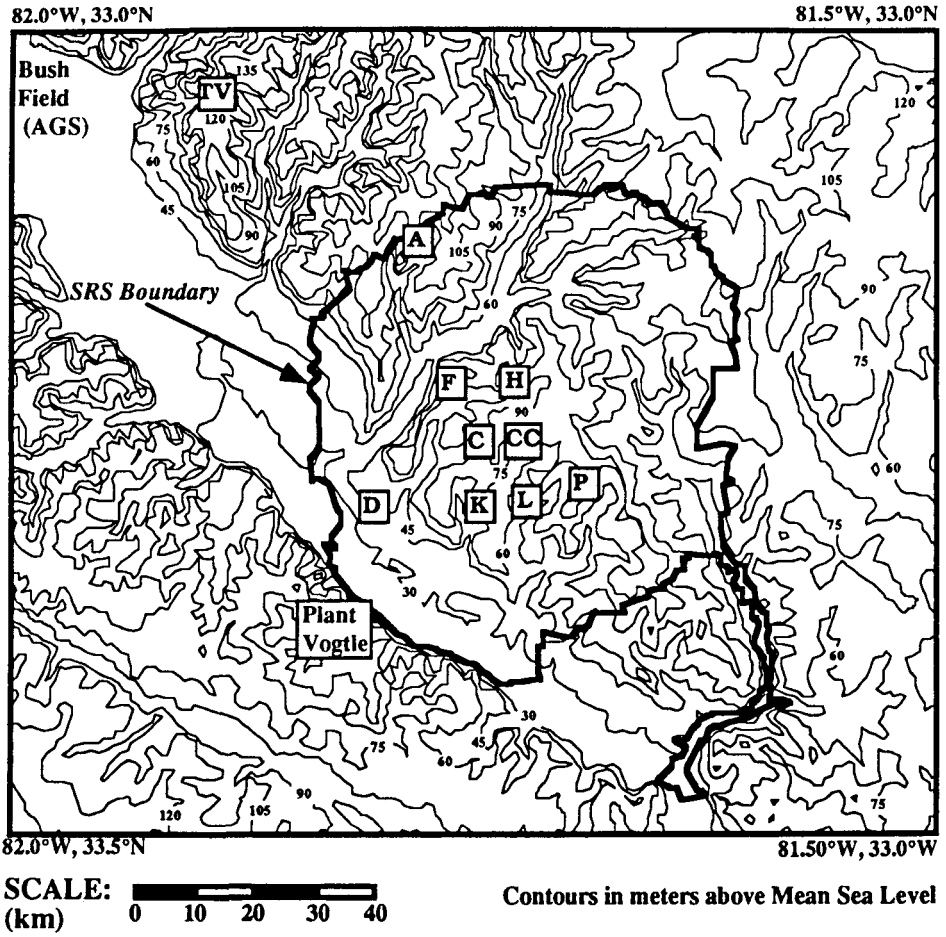

Fig. 2. Topographic map of the Savannah River Site (SRS) and surrounding area. Contours are in meters above mean sea level (MSL). Towers (capital letters), Bush Field (AGS), and Plant Vogtle sites are superimposed.

Airport (AGS) in Augusta, GA. Sodars were also located and operated by the SRTC at the CC and WJBF-TV sites (data not shown). Figure 2 gives locations and Table I describes accuracies of instrumentation used.

3. Local Terrain and Synoptic Conditions

The highest terrain at the SRS is located to the east of the Savannah River valley. Tower D is located in the flood plain. The foliage of the site varies from thickly forested 15 to 18 m deciduous trees in the flood plain to a more broken forest composed of 8 to 10 m pine and deciduous trees over the higher terrain above the

TABLE I

Accuracies of instrumentation used during project STABLE*

Manufacturer	Instrument	Variable	Accuracy
A, C, D, F, H, K, L, P 61 m			
Teledyne Geotech	Cup anemometer	Horizontal wind speed	1%
Teledyne Geotech	Bivane	Horizontal and vertical wind direction	2°
A profiles to 450 m			
AIR	Tethersonde	Horizontal wind speed	0.25 m s^{-1}
		Horizontal wind direction	5°
		Air temperature	0.5 °C
TV 18, 36, 91, 137, 182, 243, 304 m			
Climet	Cup anemometer	Horizontal wind speed	1%
Climet	Bivane	Horizontal and vertical wind direction	3°
Rosemount	Platinum resistance temperature probe	Air temperature	0.33 °C
CC 36 m			
Gill	u, v, w anemometer	Horizontal wind direction	0.03 m s^{-1}
Campbell Scientific	Sonic anemometer	Vertical wind velocity (w)	0.005 m s^{-1}
Campbell Scientific	Fine wire thermocouple	Air temperature	0.005 °C
Plant Vogtle 60 m			
Climatronics	Cup anemometer	Horizontal wind speed	1%
Climatronics	Wind vane	Horizontal wind direction	5°

* See Fig. 2 for locations of stations (A, C, D, F, H, K, L, P, TV, CC, Plant Vogtle).

flood plain. Areas not covered by forest consist of a much smaller percentage of fields, buildings, parking lots and roads, and two cooling lakes.

The synoptic condition at 0200 Eastern Daylight Time (EDT) was governed by a large high pressure system centered over central Tennessee with a stationary front located in the vicinity of northern Florida. This high pressure cell moved to North Carolina by 0800 EDT. A microbarograph trace showed variations of less than one hectopascal throughout the night. Skies were clear with little or no wind at ground level.

4. Spatial Wind Variations

The observation system of the SRS offers a unique opportunity to study the spatial variations of the wind field over a 900 km^2 area. The third night of Project STABLE offered an added unusual situation because very little large-scale pressure variation occurred which indicated no significant synoptic scale activity. Fifteen-minute averages of tower data were analyzed to depict the regional wind field.

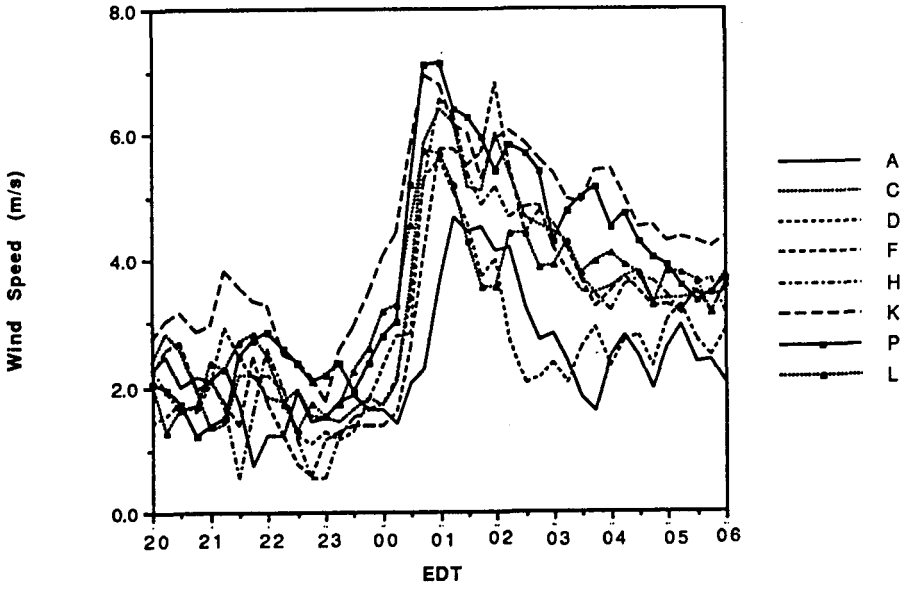

Fig. 3. Time series of 15-min averages of wind speed from the network of 61 m towers.

Figure 3 shows a time series of wind speeds measured at a height of 61 m at each of the network towers at the SRS. Wind speeds before 0000 EDT were comparatively light, but a sharp increase was observed roughly between 0000 and 0100. A closer examination of the period when the wind speed increased is shown in Figure 4 where data are plotted from towers along a north-south line extending from the TV tower south to the nearby Plant Vogtle nuclear power plant just to the west of the Savannah River. A peak in the Vogtle wind speed (single 15-min averages centered on the hour) was detected at 0000; a peak occurred at 0100 at D, after 0100 at A, and between 0030–0130 at the 91 m level of the TV tower. This implies a north-south spatial extent of at least 50 km in the observed sharp wind speed increases. Figure 5 shows data taken from the SRS towers which extend roughly east–west from D to P. All wind speed maxima were observed near 0030 with values from 5.5 to 7.3 m s^{-1}, and the east–west spatial extent was at least 30 km. The relative strength of the maxima decreased dramatically from south to north as shown by the maximum of about 8 m s^{-1} at Plant Vogtle to the minima of about 4.5 m s^{-1} at A and the TV towers.

The cause of the sharp increase in wind speed is not known. As stated above, skies were clear with very little barometric pressure change throughout the night. The NBL characteristics during this night correspond well with a Type IV night as described by Kurzeja *et al.* (1991) in a SRS climatological study of TV tower data. These nights are characterized as unsteady; that is, they begin with the normal formation of a surface inversion and then suddenly transform into a much

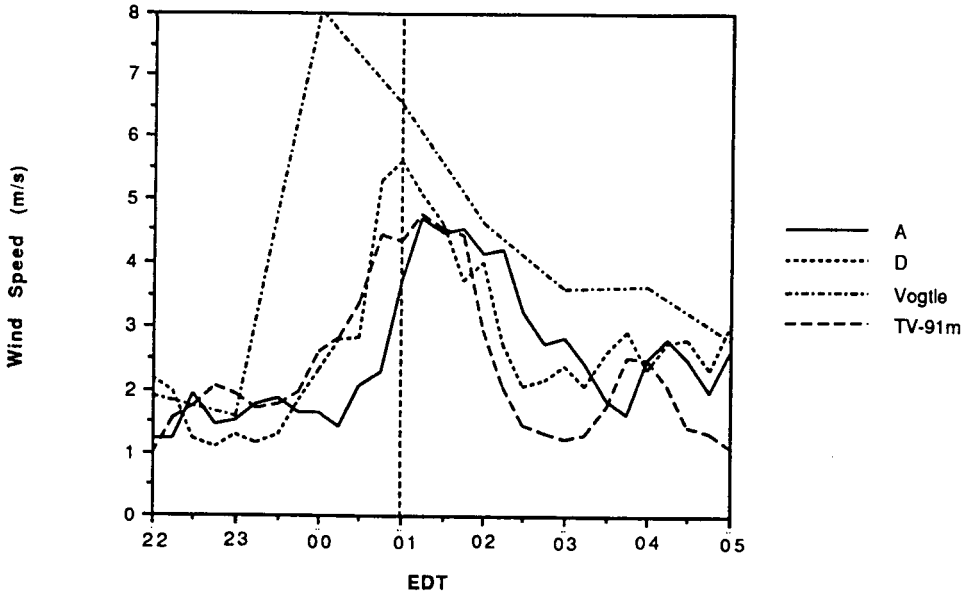

Fig. 4. Same as in Figure 3 for towers aligned north to south (Vogtle-D-A-TV).

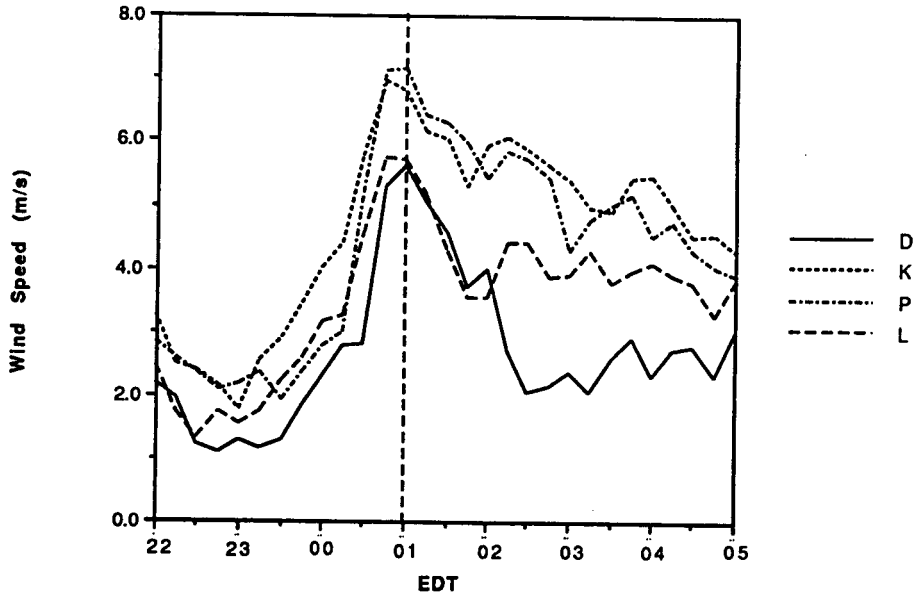

Fig. 5. Same as in Figure 3 for towers aligned west to east (D-K-L-P).

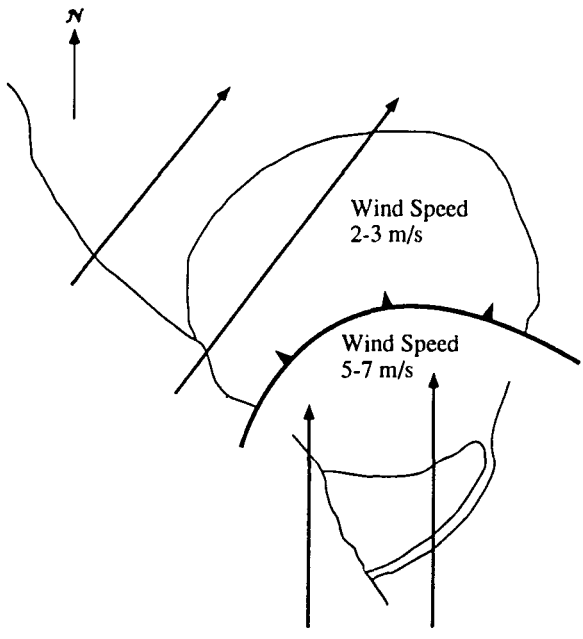

Fig. 6. Idealization of turbulent meso-flow (TMF) passing over the SRS from south to north.

more turbulent boundary layer. This transformation is associated with the passage of a "microfront", which can occur during weak prevailing pressure gradients. The term "microfront" is used very loosely since the accepted definition of a microfront (Mahrt, 1989; Stull, 1988) is associated with the passage of the backside of a large thermal in a convective boundary layer. The spatial extent of the wind speed increase is at least 30–50 km or within the meso-γ scales; however, the term "mesofront" is clearly associated with mesoscale activity such as the outflow from large complexes of thunderstorms (Schaefer *et al.*, 1986). For the purposes of this study, the phrase "turbulent meso-flow" (TMF) will be used to describe the phenomenon identified in the wind field at SRS. Weber and Kurzeja stated that a "microfront" or TMF passed over the SRS before 0000, but the present study showed that the TMF passed over the SRS between 0030 and 0130 EDT.

Surface observations from AGS, which is about 25 km to the westnorthwest of SRS, indicated very light or calm winds in the 0–2.6 m s^{-1} range with no discernible peak at 0000 EDT. Therefore, it is not clearly evident whether the TMF passed over AGS.

The dynamics of the TMF are not well understood. Figure 6 shows an idealized schematic of the TMF, shown with frontal symbols, passing south to north over the SRS at approximately 0030 EDT. The wind direction backed only 20–30° after the TMF passed. Normally, cold fronts pass from the northwest to southeast in the Southeastern United States and are accompanied by a veering wind direction.

However, the TMF moved from south to north and was accompanied by a backing wind direction. Also, the local topography suggests that drainage flows associated with terrain of the Savannah River valley would pass from northwest to southeast, not from south to north. "Microfrontal" (TMF) passage at the TV tower were shown to occur 15% or more of the time during the year (Kurzeja *et al.*, 1991). The thickness of the TMF was at least 300 m as shown in the TV tower data (see Sections 5.3 and 5.4), but the TMF probably did not extend to above a few hundred meters since there was a strong high pressure cell dominating the local weather conditions.

5. Vertical Structure of the NBL

5.1. Tethersonde profiles

As indicated above, the spatial structure of the NBL varied considerably throughout the night. To observe the vertical structure of the NBL, six launches of an instrumented tethersonde were made between 0200 and 0530 EDT at roughly half hour intervals. All of the tethersonde launches occurred after the passage of the TMF, and the launches were made near the "A" tower.

Figures 7(a), (b), (c) show the profiles of potential temperature, wind speed, and wind direction obtained at 0200, 0230, and 0300 EDT respectively; and similarly Figures 8(a), (b), (c) are for 0330, 0430 and 0530 EDT. Two wind speed maxima were observed; one just below 50 m and the other near 250 m. The lower maximum remained near $3\ m\ s^{-1}$ except for slightly higher values at 0200 EDT, which was just after the passage of the TMF. The upper level maximum dropped from a maximum of $6\ m\ s^{-1}$ to $3\ m\ s^{-1}$ as the night progressed. This decrease may have been due to the large wind shear between the upper and lower maxima which developed by 0530 EDT, but the decrease is also consistent with calculated values of wind speed based on the inertial oscillation (Stull, 1988). The calculated wind speed maximum would occur between 0100 and 0200 EDT with decreasing values the remainder of the night. Weber and Kurzeja also identified two low level wind maxima at the TV tower after the TMF had passed. The heights of the two wind speed maxima observed at the TV tower and in the tethersonde data were nearly the same. Statistically, nights with dual low-level wind maxima may occur 10–30% of the year at SRS (Kurzeja, 1991). The existence of two low level wind maxima in the lowest few hundred meters in this study differs from the expected wind speed profile over a nearly homogeneous terrain, which will usually exhibit only one wind speed maximum.

Potential temperature profiles also were significantly different from the generally observed NBL structure. Two inversions and associated stable layers were observed near 250 m and below 50 m during the night. An adiabatic layer existed between these two layers. Considerable mixing may have produced adiabatic conditions, but the thickness of this layer decreased as the night progressed. The

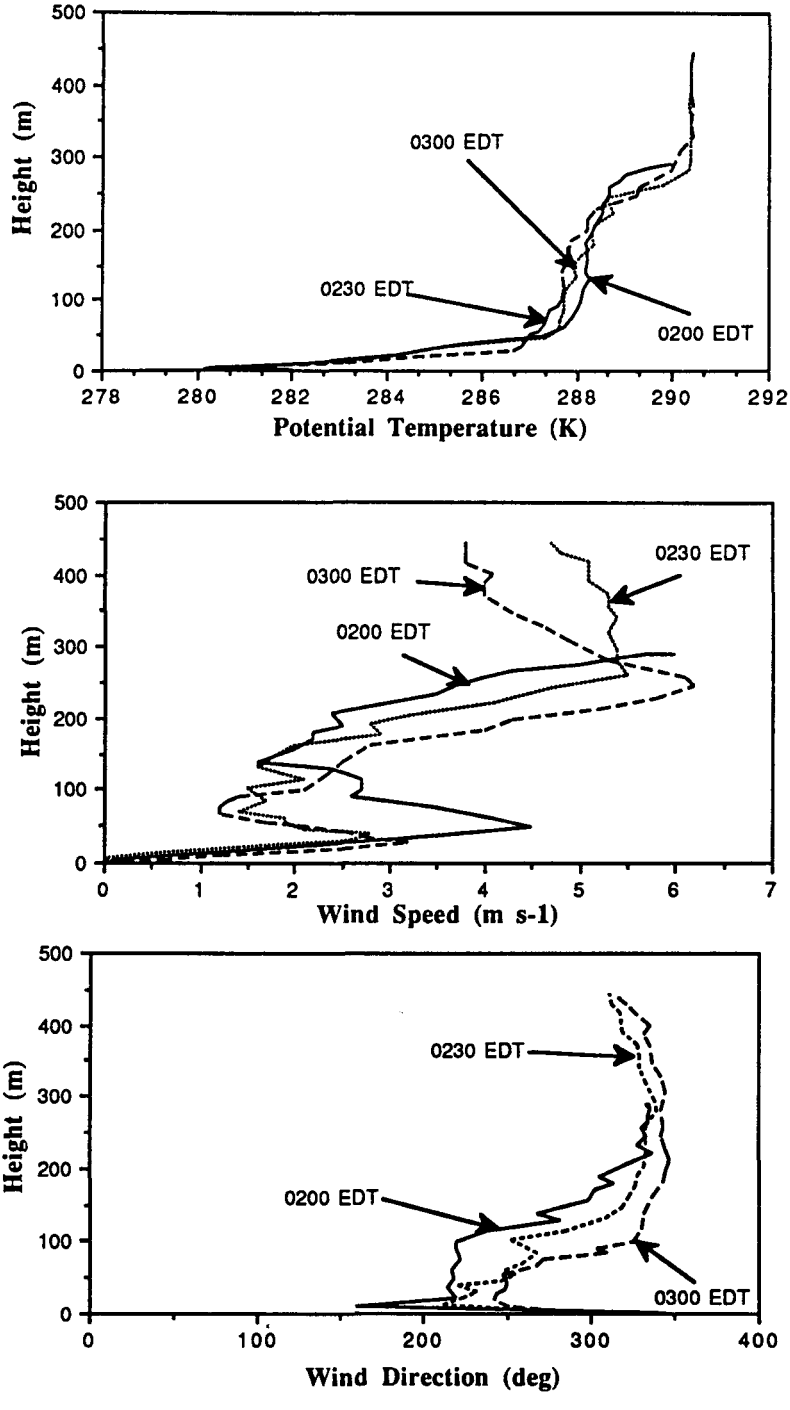

Fig. 7. (a) Profiles of potential temperature (θ, K) at 0200, 0230, and 0300 EDT; (b) same as (a) for wind speed ($m\,s^{-1}$); (c) same as (a) for wind direction (deg).

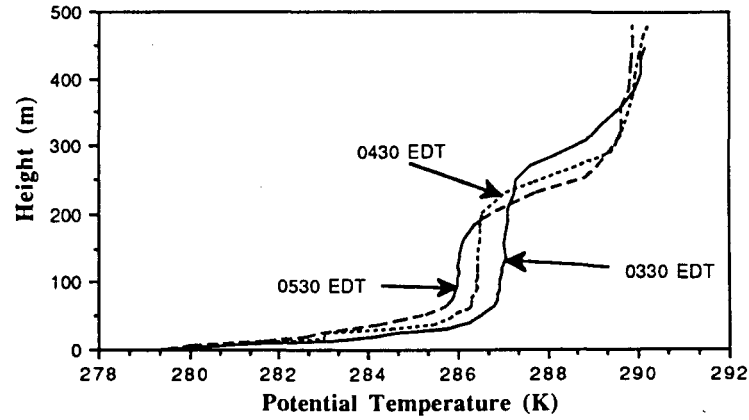

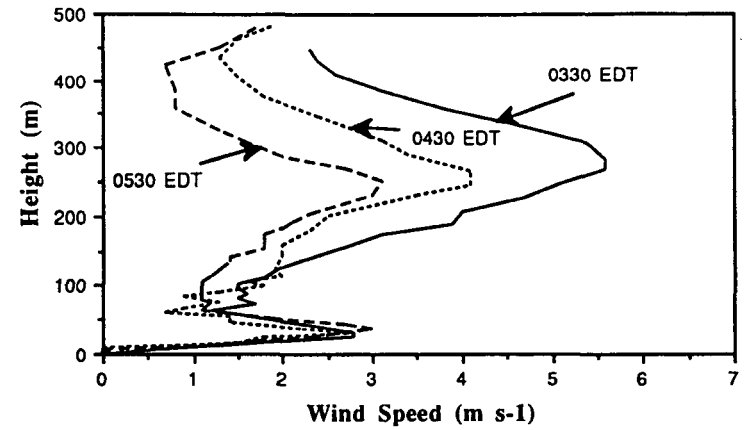

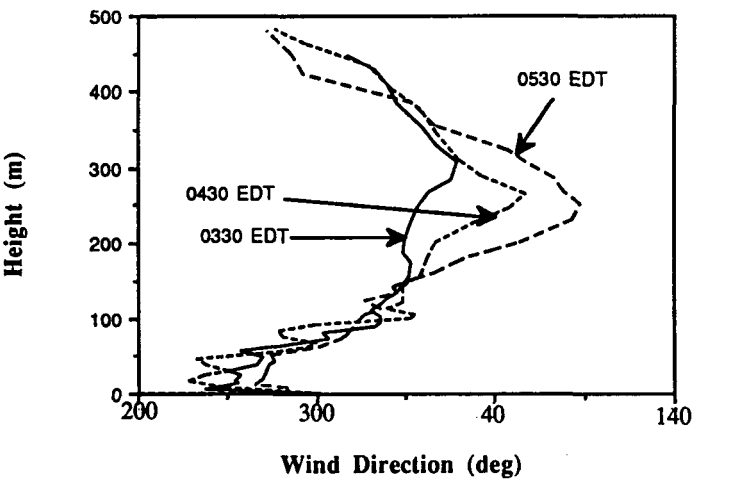

Fig. 8. (a) Profiles of potential temperature (θ, K) at 0330, 0430, and 0530 EDT; (b) same as (a) for wind speed ($m\,s^{-1}$); (c) Same as (a) for wind direction (deg).

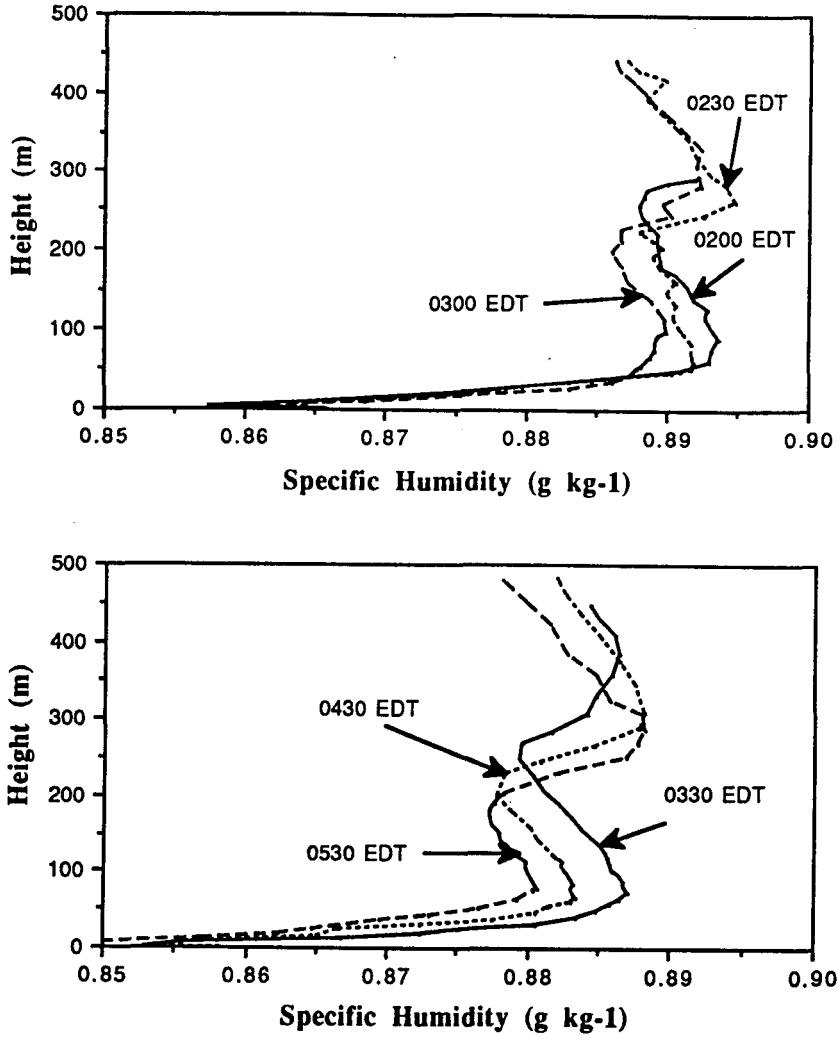

Fig. 9. (a) Profiles of specific humidity (q, g kg^{-1}) at 0200, 0230, and 0300 EDT; (b) same as (a) at 0330, 0430, and 0530 EDT.

upper level (250 m) wind maximum generally was located just above the upper level inversion even as the height decreased. The height of the lower level wind maximum was slightly below the height of the lower inversion and remained in this relative position throughout the remainder of the night. A general cooling trend was also observed. Typical NBL profiles show the existence of a ground-based inversion as opposed to the ground-based inversion and an elevated inversion with an active turbulent layer observed in this study.

A similar "dual" nature was also noted in the specific humidity profiles shown in Figures 9(a), (b). All six profiles showed a dual peak behavior with the lower

maxima located at 80 m except the profile at 0200 EDT when the launch was terminated at 300 m. The heights of the lower level wind maxima and the height of the surface-based inversion were located below the level of the specific humidity peak. The lower level maximum may have been induced by a sink created by the condensation of moisture in the form of dew at the ground surface (Arya, 1988). This moisture sink created by surface condensation induced a peak just above the stable layer at the surface. The observed upper level specific humidity peaks were generally located just above the upper level (250 m) inversion identified in the potential temperature profiles. Specific humidity minima were located within the adiabatic layer located between the two stable layers identified by the potential temperature profiles. The adiabatic layer also may have acted as a sink for moisture in the NBL. This second sink for moisture induced another specific humidity maximum above the adiabatic layer. Or, the complex moisture profiles may have been influenced by the origin of the air in each layer since the strong wind direction shear with height may have enhanced the transport of moisture from distant locations.

5.2. Richardson number contours from tethersonde data

The fine vertical resolution of the tethersonde data provides an opportunity to study the turbulent characteristics of the NBL. Contours of the gradient Richardson number, Ri, obtained from tethersonde data for the period 0230 to 0530 EDT are shown in Figure 10. Ri was calculated using:

$$\mathrm{Ri} = [(g/\bar{\theta})\,\partial\bar{\theta}/\partial z][(\partial\bar{u}/\partial z)^2 + (\partial\bar{v}/\partial z)^2]^{-1},$$

where g is acceleration due to gravity, $\bar{\theta}$ is mean potential temperature of the layer, and $\bar{u}$, $\bar{v}$ are mean horizontal wind components.

The flow was generally nearly laminar ($\mathrm{Ri} > 0.5$) above 250 m. Similar values were also observed below 50 m. A more turbulent layer is indicated by values of $\mathrm{Ri} < 0.25$ between the upper and lower stable layers. "Pockets" of stronger turbulence ($\mathrm{Ri} < 0$) were observed at varying heights before 0430 EDT. The thickness of the turbulent layer between the upper and lower inversions showed a decreasing trend from about 150 m to only 50 m by 0600 EDT. This could have been due to the increasing stability of the NBL as the surface continued to cool.

Despite differences in temporal and spatial resolutions, the tethersonde Ri contours correspond well with Ri contours obtained after 0000 EDT from 1 min averages of the TV tower observations (Weber and Kurzeja, 1991). The persistent turbulent layer sandwiched between the stable layers was shown to exist at the TV tower and the tethersonde launch sites after the passage of the TMF, which implies a spatial extent of at least 30 km. Turbulent episodes extending to the surface were observed at the TV tower at 0150 and 0345 EDT but were not detected by the tethersonde data, which may have been due to the relatively coarse time resolution of the tethersonde data compared to the TV tower data (30 min to 1 min) and to the different measuring sites which were 30 km apart.

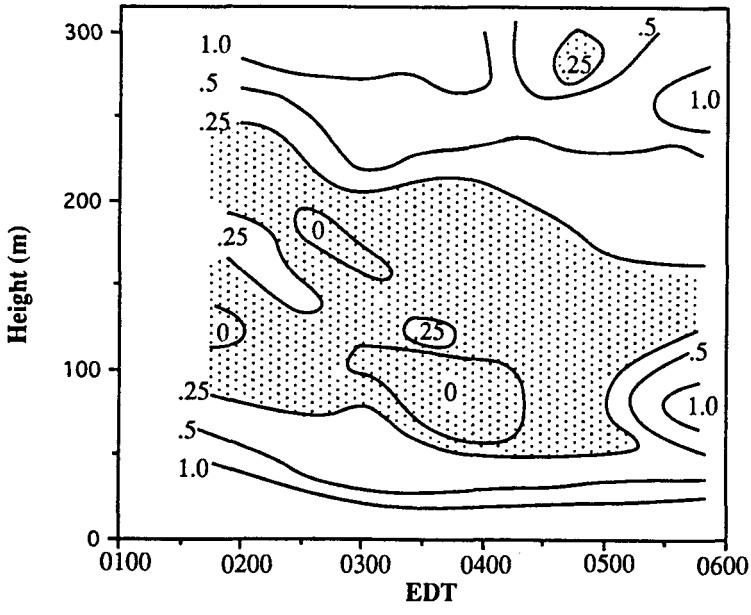

Fig. 10. Time-height contours of Richardson number from tethersonde data. Shaded areas indicate higher turbulence.

The effect of the passage of the TMF on the structure of the NBL was not shown by the tethersonde data since the experiment began at 0000 EDT.

5.3. Time histories of air temperature from the TV tower

Time series of air temperatures with averaging periods in the order of seconds can reveal additional micrometeorological features. The amount of information gained is enhanced considerably by concurrent time histories at different levels in the boundary layer. The TV tower is instrumented with slow response temperature probes (with a time constant of about 5 s) at seven levels (18, 36, 91, 137, 182, 243, and 304 m), from which 5-sec averages were created. The time series at these levels are shown in Figures 11(a), (b).

Two general features are apparent from these figures. A general cooling trend is evident at all levels as the night progressed. The second feature is a sharp discontinuity just after 0030 EDT. This discontinuity involved a significant (2–4 °C) drop in temperature associated with the passage of the TMF.

Other relevant information on the turbulence characteristics of the NBL can also be deduced from the time histories of air temperature. Often, during strongly stable conditions, temperature time series show the existence of internal gravity waves (Sethu Raman, 1977, 1980) as seen at the 304, 243, 36, and 18 m levels. However, the 91, 137, and 182 m levels exhibited the presence of few or no gravity waves. These three traces indicated the presence of an elevated adiabatic layer

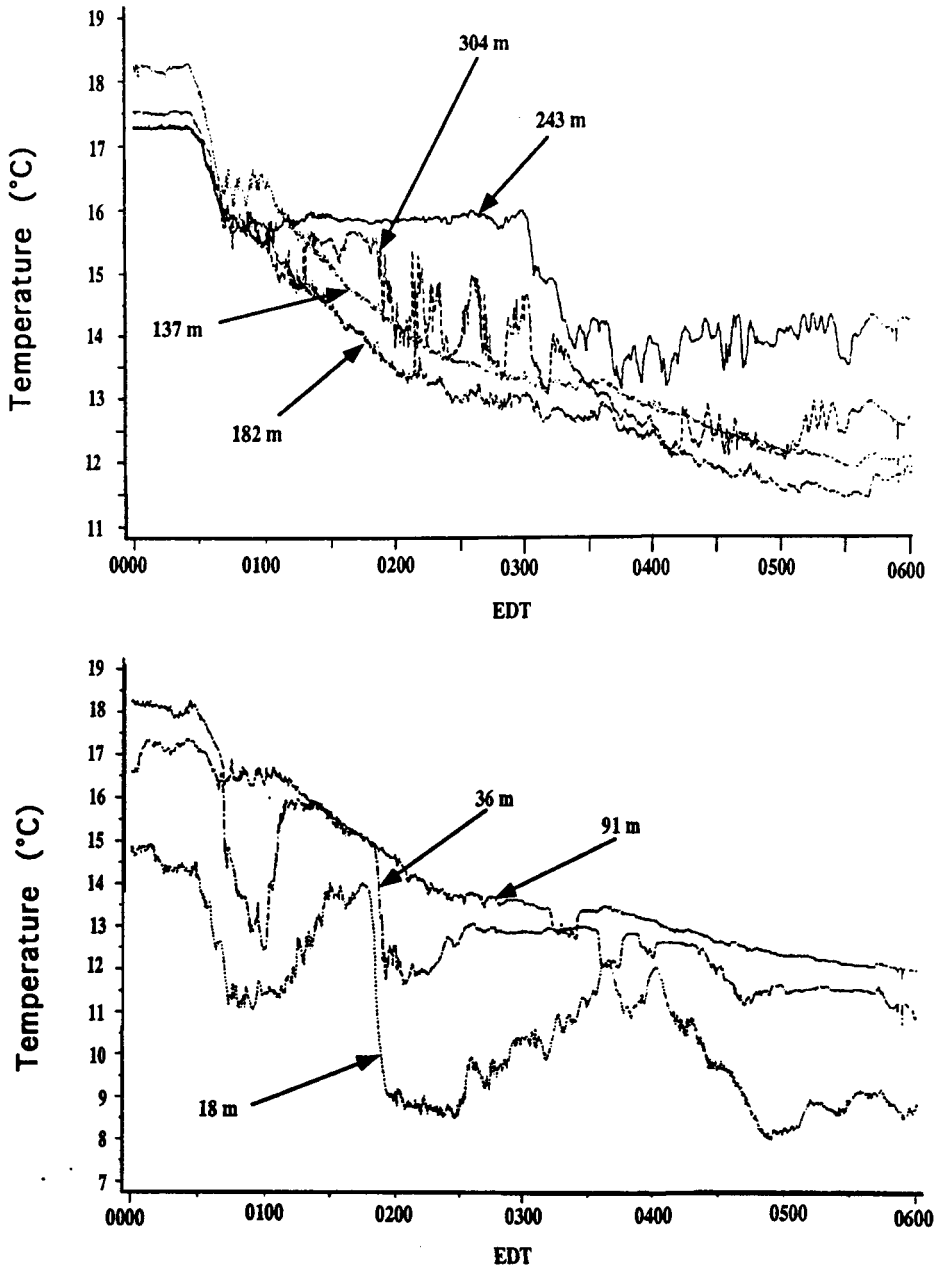

Fig. 11. (a) Time histories of 5-sec averages of air temperature (°C) at 304, 243, 182, and 137 m.

with active turbulence throughout the night. The layer between 200 m and 300 m and the layer below 100 m were stable and much less turbulent. (The elevated adiabatic layer was also indicated by the tethersonde data, see Sections 5.1 and 5.2).

5.4. Time histories of wind speed from the TV tower

Wind speed traces yield similar turbulence information. Figures 12(a), (b) show 5-sec average time series of wind speeds obtained from cup anemometers located at the same levels as the temperature probes. In both plots, three distinctly different periods of activity can be seen. The early part of the night between 2100 and 0030 EDT was relatively "calm" with only small variations. The period between 0030 and 0200 EDT featured a sharp increase in wind speed with large velocity fluctuations in association with the passage of the TMF. As shown in Section 5.3, a corresponding sharp drop in temperature also occurred during this period. Such wind and temperature discontinuities commonly occur during the passage of a synoptic-scale cold front. However, these variations occurred without the presence of a synoptic cold front, under clear conditions, and with no discernible discontinuity in the microbarograph pressure trace. Only a moderate (20–30°) veering trend of wind direction (see Figure 6) was noted. The period after the passage of the TMF between 0230 and 0600 EDT was less turbulent. The wind speed and temperature traces both exhibit characteristics which are consistent with internal gravity waves with turbulence superimposed (Sethu Raman, 1977, 1980).

5.5. Richardson number contours from TV tower data

Figure 13 shows the Ri contours calculated from 15-min averages of TV tower data. Shaded areas indicate values below 0.25, when conditions are presumed to be turbulent. Residual daytime turbulence existed between 100–180 m well after sunset until about 0000 EDT. The persistent adiabatic layer between 75–200 m which was identified by the tethersonde and TV tower data existed throughout the entire night. The TMF which passed the TV tower near 0030 had little effect on the values of the Richardson Numbers although a turbulent period was noted from 0100 to 0200 between about 100–180 m. Two turbulent periods which may have reached the surface were observed at 0330 and 0450.

6. Structure of NBL Turbulence

6.1. Turbulent heat fluxes

Time histories of the turbulent sensible heat flux [H(W m^{-1})] as well as σ_W, σ_T, and σ_A, measured at the 36 m level of the CC tower for the entire night are shown in Figure 14. Normally, in the stable NBL over flat terrain, the sensible heat flux is most negative near the earth's surface and changes rapidly to near zero at the top of the NBL. From 2100 to 0000 EDT, the heat flux at 36 m was very nearly

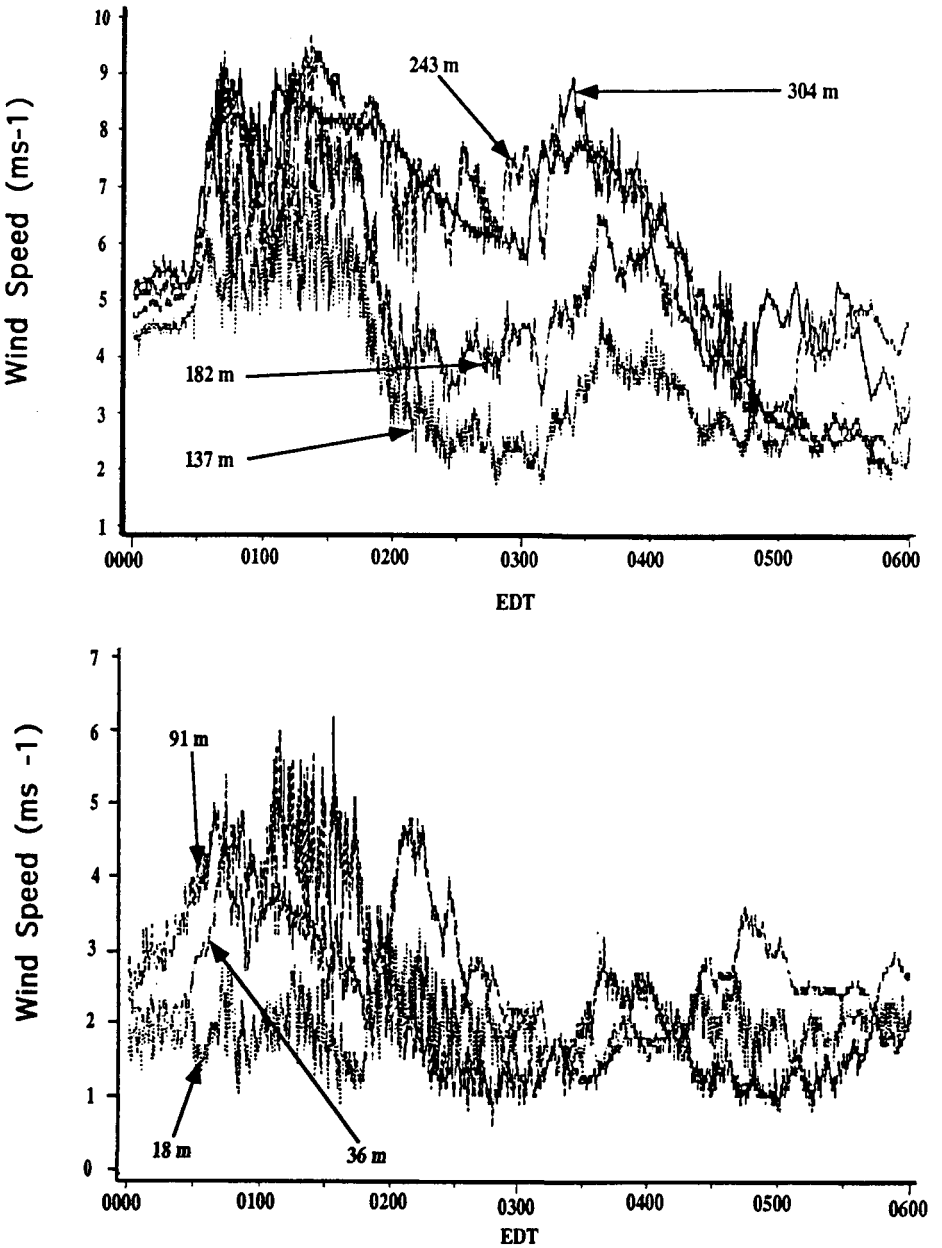

Fig. 12. (a) Time histories of 5-sec averages of wind speed ($m\,s^{-1}$) at 304, 243, 182 and 137 m; (b) same as (a) except at 91, 36 and 18 m.

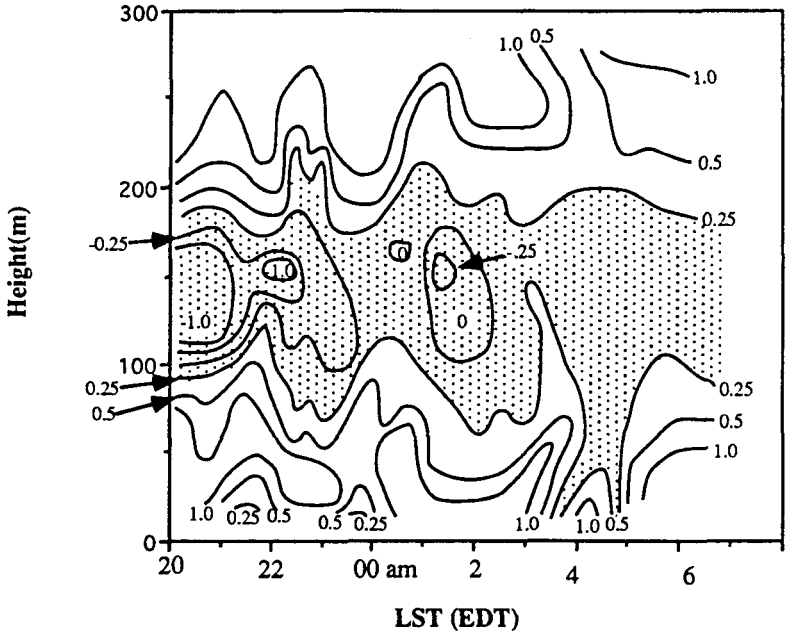

Fig. 13. Time-height contours of Richardson number from 15-min averages of TV tower data. Shaded areas indicate higher turbulence.

zero. A sharp decrease at 0100 and 0200 EDT indicates that enhanced cooling occurred due to the turbulence observed during the passage of the TMF at about 0030 EDT. Standard deviations of temperature and vertical velocity also exhibited peaks at 0100 EDT. Near-zero values of H were observed for the remainder of the night.

Since near-zero values for the heat flux are normally found at the top of the NBL, it is likely that 36 m was near the top of the NBL. The low-level wind maximum and the lowest stable layer observed near 50 m in the tethersonde and TV tower data also suggest that the depth of the NBL was only about 36 m. However, the elevated turbulent layer above 50 m probably interacted with the NBL for short periods as indicated by the profiles of Ri from the TV tower (Figure 13).

6.2. Standard deviations

Figure 14 shows that maxima of σ_W and σ_T were observed during the same periods (0100 to 0200 EDT) as the H maxima (which immediately followed the passage of the TMF). Standard deviations of horizontal wind direction (σ_A) were nearly constant except for the two peaks at 2100 and 0200 EDT. The 0200 EDT peak may be due to the wind shift after the passage of the TMF. The peak at 2100 EDT may have been associated with residual turbulence from the daytime atmospheric boundary layer or with light winds following the evening transition period.

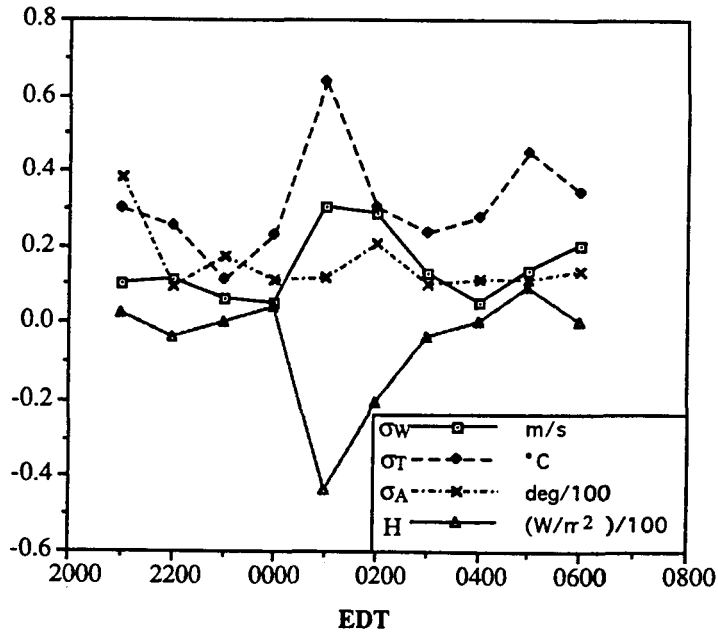

Fig. 14. Hourly averages of the standard deviations of vertical velocity (σ_W, m s^{-1}), air temperature (σ_T, °C), wind direction (σ_A, deg), and of turbulent heat flux [(H, (W m^{-2})]. Observations made at 36 m.

It is interesting to note that both σ_T and σ_W showed secondary peaks at 0500 and 0600 EDT. Surprisingly, little variation of σ_A was observed between 0300 to 0600 EDT when wind speeds were lighter (2.5 m s^{-1}).

6.3. Spectra

Turbulence spectra for the temperature fluctuations obtained by the fine wire thermocouple probe at 0300 and 0600 EDT are shown in Figures 15(a), (b) as functions of normalized frequency (nz/U). The spectra correspond to 20–25 min sampling periods well after the TMF had passed the CC tower. The spectra show that the maximum energy amplitude decreased due to increasing stability (see Figures 10 and 13), which reduced the size of the energy-containing eddies between 0300 and 0600 EDT. The small peaks in these spectra suggest the presence of internal gravity waves with dominant wavelengths of about 55 and 80 m at 0300 and 0600 EDT, respectively. The associated wave periods (20–35 s) are less than the maximum wave period expected using an estimate (110 s) of the Brunt–Vaisala frequncy (Weber and Kurzeja, 1991). However, the peaks may not be significant since only a limited number of spectra were calculated.

Comparing Figures 15(a), (b) with an idealized spectra shown by Hunt *et al.* (1983), "weak" to "moderate" wave activity was observed. In general, the two

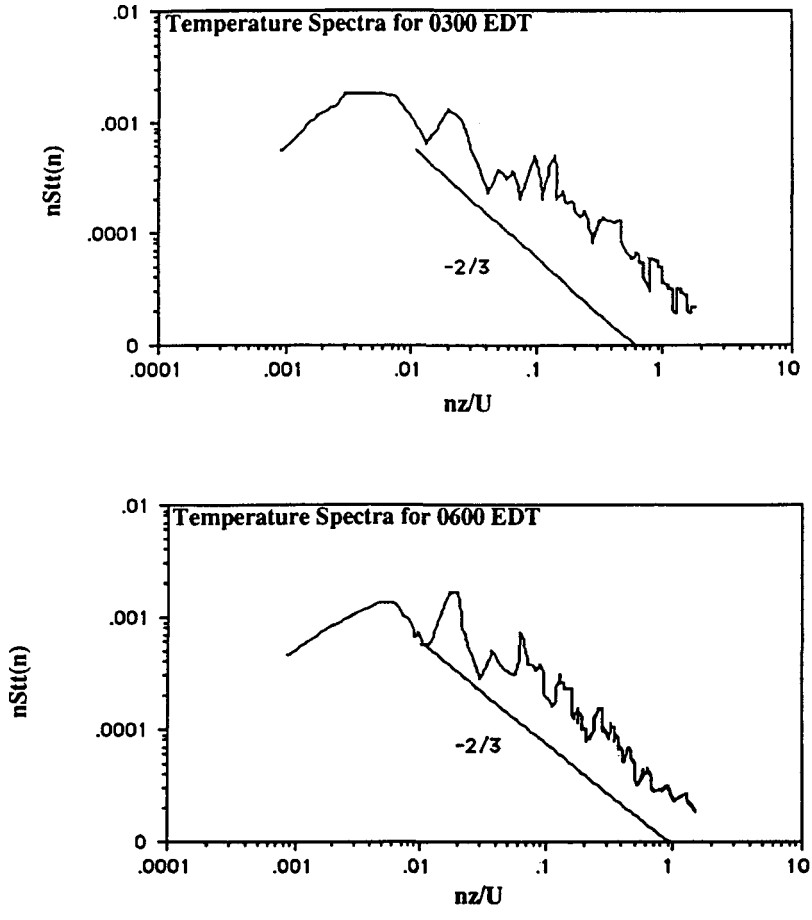

Fig. 15. (a) Temperature spectrum observed at 0300 EDT at 36 m; (b) same as (a) except for 0600 EDT.

spectra show similar behavior which is characteristic of eddies normally found in the stably stratified NBL (Caughey *et al.*, 1979). These spectra corroborate the conclusion that the 36 m level at the CC tower was located within the stable layer associated with the surface inversion, and may also indicate that internal gravity waves were present in the NBL after the passage of the TMF.

7. Composite Structure

Figure 16 shows a composite of the structure of the lowest few hundred meters for the entire night. Residual daytime turbulence (1) was observed until about 2100 EDT. A ground-based inversion (2) developed soon after sunset and rose to 50 m by 2300 EDT, and a weak inversion (3) formed near 250 m by 1930 EDT.

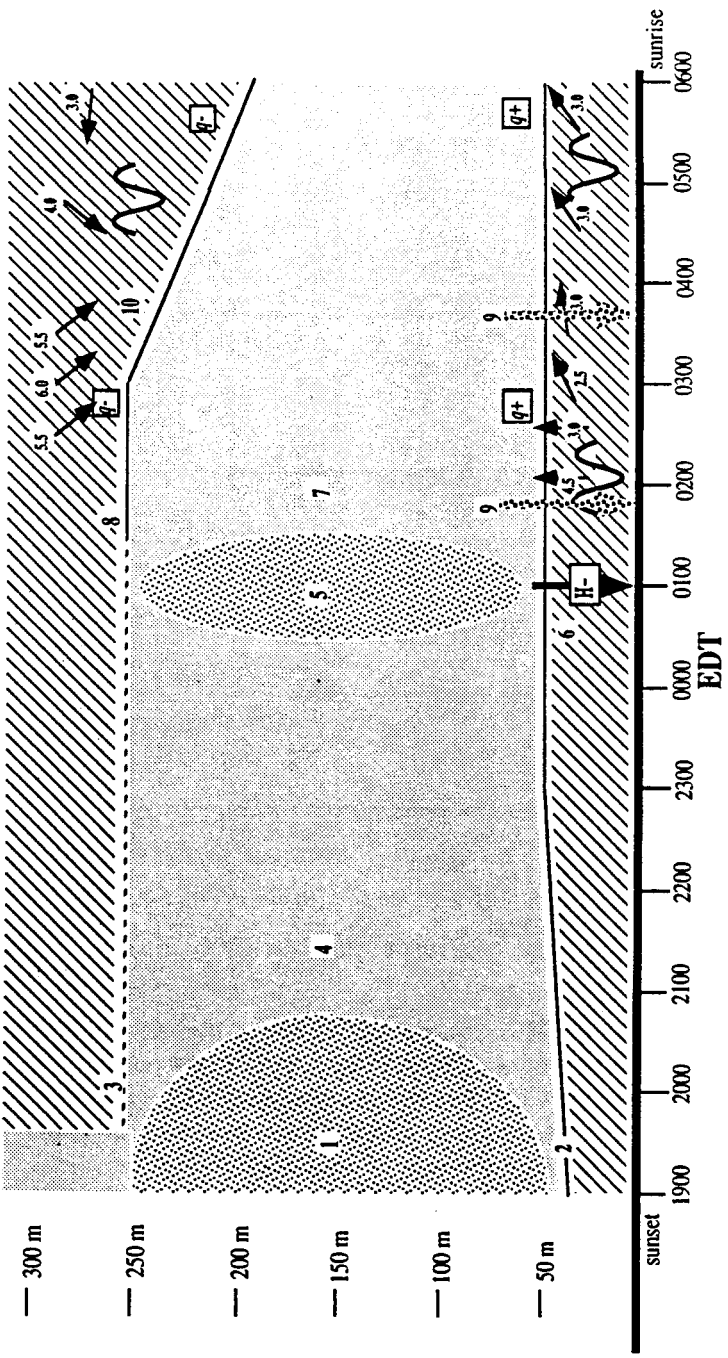

Fig. 16. Schematic of the composite structure of the nocturnal planetary boundary layer during the third night of Project STABLE.

A stable layer existed above the upper and below the lower inversions. An elevated turbulent layer (4) existed between the two stable layers through the entire night. Near 0100 EDT, increased turbulence was observed (5) during the passage of a TMF with considerable cooling at the lower levels as evidenced by the negative heat flux (6). Turbulence decreased in intensity between stable layers (7) but nevertheless continued – possibly due to shear instability. The upper inversion (8) strengthened and remained near 250 m, and internal gravity waves ($\wedge\vee$) became evident above 250 m and below 50 m. A low level jet formed just below 50 m at 0200 EDT, and an upper jet formed near 270 m by 0230 EDT. Turbulent episodes which reached the surface (9) were observed at 0150 and 0345 EDT. Specific humidity maxima ($q+$) were observed just above the lower inversion, and minima ($q-$) just above the upper inversion during each of the six tethersonde runs. The upper level inversion (10) began sinking at 0300 EDT as the elevated turbulent layer decreased in thickness to about 150 m by sunrise.

8. Conclusions

The third night of Project STABLE (1988) at the Savannah River Site (SRS), exhibited many interesting nocturnal boundary-layer (NBL) features. The passage of a mesoscale phenomenon, defined as a turbulent meso-flow (TMF), is described and a composite structure of the lowest few hundred meters over complex terrain is presented.

The spatial extent of the TMF was at least 30–50 km, but the forcing is not well understood since the TMF occurred without the presence of a synoptic-scale cold front, under clear conditions, and with no discernible discontinuity in a microbarograph pressure trace.

The composite structure of the lowest few hundred meters over the complex terrain at the Savannah River Site differed from that expected over homogeneous terrain. The composite structure consisted of dual low-level wind maxima, dual inversions, and a persistent, elevated turbulent layer. This latter layer, previously identified from instrumentation located on a 304 m tower, was shown from tethersonde data in the present study to have had a spatial extent of at least 30 km. Richardson number time-height contours calculated from 15-min data for the entire night showed that the elevated turbulent layer existed from sunset to sunrise. Internal gravity waves were suggested to exist in the stable layers above and below this turbulent layer. The persistent adiabatic layer may have resulted from turbulence induced by shear instability.

Acknowledgments

The authors would like to acknowledge the support provided by the Savannah River Technology Center and NCSU during and after the experiment. In particular, thanks to A. H. Weber, R. J. Kurzeja, and R. P. Addis of SRTC for

document review and comments. Thanks to S. P. S. Arya of NCSU for his suggestions in data analysis and Brian and Suzanne Templeman who also took part in the experiment. Finally, appreciation is given to Plant Vogtle of the Georgia Power Company for providing tower data.

This work was supported by the National Science Foundation under INT-82-19710 and ATM-8801650, while the primary author was a graduate student at NCSU, and by Contract No. DE-AC09-89SR18035 with the U.S. Department of Energy.

References

Arya, S. P. S.: 1988, *Introduction to Micrometeorology*, Academic Press, Inc., New York. 307 pp.

Caughey, S. J., Wyngaard, J. C. and Kaimal, J. C.: 1979, 'Turbulence in the Evolving Stable Boundary Layer', *J. Atmos. Sci.* **36**, 1041–1052.

Hunt, J. C. R., Kaimal, J. C., Gaynor, J. E. and Korrell, A.: 1983, 'Observations of Turbulence Structure in Stable Layers at the Boulder Atmospheric Observatory', in J. C. Kaimal (ed.), *Studies of Nocturnal Stable Layers at BAO*. Report #4, NOAA/ERL Boulder, Colorado. 129 pp.

Kurzeja, R. J., Berman, S. and Weber, A. H.: 1991, 'A Climatological Study of the Nocturnal Planetary Boundary Layer', *Boundary-Layer Meteorol.* **54**, 105–128.

Mahrt, L.: 1989, 'Intermittency of Atmospheric Turbulence', *J. Atmos. Sci.* **46**, 79–95.

Schaefer, J. T., Hoxit, L. R. and Chappell, C. F.: 1986, 'Thunderstorms and Their Mesoscale Environment', in E. Kessler (ed.), *Thunderstorm Morphology and Dynamics*, University of Oklahoma Press, Norman, OK, 411 pp.

SethuRaman, S.: 1977, 'The Observed Generation and Breaking of Atmospheric Internal Gravity Waves Over the Ocean', *Boundary-Layer Meteorol.* **12**, 331–349.

SethuRaman, S.: 1980, 'A Case of Persistent Breaking of Internal Gravity Waves in the Atmospheric Surface Layer Over the Ocean', *Boundary-Layer Meteorol.* **19**, 67–80.

Stull, R. B.: 1988, *An Introduction to Boundary Layer Meteorology*, Kluwer Academic Publishers, Boston. 665 pp.

Weber, A. H., and Kurzeja, R. J.: 1991, 'Nocturnal Planetary Boundary Layer Structure and Turbulence Episodes During the Project STABLE Field Program', *J. Appl. Meteorol.* **30**, 1117–1133.